

# Open cell semi-rigid polyurethane foams synthesized using palm oil-based bio-polyol



N.E. Marcovich<sup>a</sup>, M. Kurańska<sup>b,\*</sup>, A. Prociak<sup>b</sup>, E. Malewska<sup>b</sup>, K. Kulpa<sup>b</sup>

<sup>a</sup> Institute of Material Science and Technology (INTEMA), National University of Mar del Plata, Mar del Plata, Argentina

<sup>b</sup> Cracow University of Technology, Department of Chemistry and Technology of Polymers, Cracow, Poland

## ARTICLE INFO

### Article history:

Received 15 October 2016

Received in revised form 15 March 2017

Accepted 17 March 2017

### Keywords:

Semi-rigid polyurethane foams

Palm oil-based polyol

Heat insulating materials

## ABSTRACT

Semi-rigid polyurethane foams were successfully prepared by blending up to 70 wt.% of a palm oil-based bio-polyol with a petrochemical polyether polyol. Due to the high viscosity of the bio-polyol derived from palm oil, polyol premixes were heated before mixing with an isocyanate component. Despite this, a slowdown in the foaming and gelling reactions was detected as the content of the palm oil-based bio-polyol in the formulation increased. The thermal conductivity of the modified foams was higher than that of the reference one, even when they exhibited a lower apparent density. In addition, their mechanical and dynamic mechanical properties decreased as the palm oil-based polyol content in the final foams increased. These effects are attributed to the foams' cellular structure since the closed cell content decreased as the amount of the petrochemical polyol replaced by the bio-polyol increased. However, the water absorption decreased as the bio-polyol concentration in the polyurethane formulation increased and the modified foams exhibited excellent dimensional stability. Taking into account potential applications of polyurethane systems, the formulation containing 30 wt.% of the bio-polyol could be used in the preparation of a new generation open cell semi-rigid foams permeable to moisture and with higher content of biomass-derived constituents.

© 2017 Elsevier B.V. All rights reserved.

## 1. Introduction

The synthesis of polymers based on natural components is one of the most important fields in the current research and development for the environmental protection (Tanaka et al., 2008; Cateto et al., 2011; Oliveira et al., 2015). Studies on polyurethanes (PURs) based on components from natural resources have a great potential in contributing to the development of this area (Calvo-Correas et al., 2016). PURs are obtained through the reaction of polyols and isocyanates. Nowadays, commercial isocyanates and polyols for the synthesis of PUR foams are mostly derived from petroleum. However, a trend to use components based on renewable resources is observed in research works (Zhou et al., 2015). Among such raw materials, mostly petrochemical polyols are partially or even fully replaced by bio-polyols, especially those derived from natural oils, starch, sugar and lignin (Yao et al., 1996; Cateto et al., 2009; Hakim et al., 2011; Seydibeyoglu et al., 2013; D'Souza et al., 2014; Paberza et al., 2014; Bernardini et al., 2015; Arshanska et al., 2016). Thus, there have been many reports on synthesizing PUR foams using

bio-based polyols from various vegetable oils such as palm (Tanaka et al., 2008; Pawlik and Prociak, 2012; Zeimaran et al., 2013), soy (Campanella et al., 2009), linseed (Calvo-Correas et al., 2015), rapeseed (Prociak and Rojek, 2012; Kirpluks et al., 2013; Kurańska et al., 2015a,b), tung (Mosiewicki et al., 2008; Soto et al., 2016) and castor oil (Mosiewicki et al., 2009; Gomez-Fernandez et al., 2016). Palm oil is one of the most important vegetable oils due to its price and production efficiency in comparison to any other commercial oils. The production of crude palm oil in Malaysia was approximately 19.22 million tonnes in 2014 (Arniza et al., 2015).

Palm oil-based bio-polyols can be obtained by an introduction of hydroxyl groups into the positions of double bonds or ester bonds. Several methods, such as epoxidation followed by opening of oxirane rings using various compounds with active hydrogen atoms, hydroformylation, ozonolysis and hydrogenation, transesterification and transamidization, can be used in their synthesis. These different methods of converting natural oils into bio-polyols allow obtaining hydroxyl derivatives characterized by various chemical structures. The structure of polyols has a significant influence on the final properties of PUR foams, which also depend on the foaming process conditions (Arbenz et al., 2016).

Kurańska and Prociak (2016) analyzed the foaming process of water-blown PUR foams with different contents of rapeseed

\* Corresponding author.

E-mail address: [maria.kuranska@gmail.com](mailto:maria.kuranska@gmail.com) (M. Kurańska).

oil-based polyols. They concluded that a replacement of a petrochemical polyol with a rapeseed oil-based polyol had a significant effect on the foaming process by reducing the reactivity of the PUR system. The foaming process was analyzed using a FOAMAT® system, a device that allows analyzing the dielectric polarization of reaction mixtures (among others), which reflects the conversion degree of functional groups during the PUR formation. A modification of the reference PUR system based on a petrochemical polyol by replacing the petrochemical polyol with rapeseed oil-based hydroxyl derivatives resulted in a smaller decrease in the dielectric polarization which reflects slower gelling and foaming reactions.

Bio-polyols can be used for a preparation of different types of PUR materials including flexible and rigid foams. An addition of natural raw materials can change both the physical and chemical properties of PUR foams and result in a more ordered cellular structure of the modified foams than in the case of the reference material, as was reported in several papers (Pawlak and Prociak, 2012; Prociak et al., 2012).

Bio-polyols used to obtain flexible foams usually have a hydroxyl number in the range of 50–200 mgKOH/g (Campanella et al., 2009; Prociak and Rojek, 2012; Zhang and Kessler, 2015). Flexible foams obtained with palm oil-based bio-polyols have a generally higher apparent density than the reference foams. Moreover, it turned out that the mechanical properties of the materials modified had been improved. The foams with an addition of 15% of the bio-polyol had almost twice the tensile strength and three times higher compressive stress at 40% strain in comparison to the petrochemical foams. The foams' resilience increased with an increasing bio-polyol addition (Pawlak and Prociak, 2012; Prociak et al., 2012). The cellular structure of the foams was also influenced when a rapeseed oil-based bio-polyol was used as the replacement of a petrochemical polyol resulting in smaller cell sizes as the amount of the bio-polyol increased. In this case, it was also observed that the mechanical properties of the foams prepared depended on the concentration of the rapeseed oil-based polyol: the introduction of the rapeseed oil-based polyol to the PUR formulation increased the apparent density (as in the case of the palm oil-based bio-polyol), but reduced the hardness and resilience of the final foams. What is more, the foams modified with the rapeseed oil-based bio-polyol had a higher value of support factor in comparison to the reference foam (Malewska et al., 2015; Prociak et al., 2015).

Bio-polyols used to obtain rigid PUR foams usually have a hydroxyl number in the range of 250–400 mgKOH/g (Lee et al., 2007; Kurańska et al., 2015a,b; Zieleniewska et al., 2015). Such foams obtained with bio-polyols have properties similar to commercial materials and can be used, for example, as heat insulating materials. A replacement of a petrochemical polyol with rapeseed oil derivatives is possible even up to 80 wt.% and their use can have a beneficial influence on the heat insulating properties of such bio-foams, as reported in several papers (Kurańska et al., 2013; Arniza et al., 2015).

Most often, rigid PUR foams are characterized by closed cell structures. Such materials have excellent thermal insulating properties due to a gas (blowing agent) enclosed in their structures. Such PUR foams have the highest resistance to heat flow among commercially available thermal insulating materials. The chemical structure of PUR materials provides effective air barrier, low moisture vapour permeability and resistance to water.

Nowadays, an increase in the people's interest in the application of rigid and semi-rigid PUR foams with an open cell structure as heat insulating building materials is noticeable. This type of materials is permeable to moisture, has a lower apparent density and as a consequence is cheaper. However, their thermal conductivity is higher in comparison to closed cell foams.

**Table 1**  
Formulations of semi-rigid foams modified with palm oil polyol.

Component	REF	PP10	PP30	PP50	PP70	PP100
<b>Component A</b>						
RF 551	100	90	70	50	30	0
PP102	0	10	30	50	70	100
Water	4.5	4.5	4.5	4.5	4.5	4.5
Polycat 9	1.8	1.8	1.8	1.8	1.8	1.8
L6915	1.5	1.5	1.5	1.5	1.5	1.5
<b>Component B</b>						
p-MDI	188.4	179.9	162.5	145.6	128.7	103.3

In the scientific literature, open cell semi-rigid and rigid PUR foams are described very rarely. Therefore, an application of bio-based components in PUR systems for the production of open cell semi-rigid foams should be interesting.

In this paper, a palm oil-based polyol was obtained and characterized in order to be further used to modify a PUR formulation to produce semi-rigid foams. Both the foaming process and selected properties of the PUR foams modified are discussed.

## 2. Experimental

### 2.1. Materials and methods

A petrochemical polyether polyol Rokopol RF-551 with a hydroxyl value of 449 mgKOH/g was supplied by PCC Rokita SA.

A palm oil-based bio-polyol was prepared in the Department of Chemistry and Technology of Polymers in Cracow University of Technology. The bio-polyol was synthesized by the epoxidation of palm oil at 60 °C using performic acid generated in situ by the reaction of hydrogen peroxide ( $H_2O_2$ ) with a formic acid followed by ring opening with  $H_2O$  in the presence of a concentrated sulfuric acid as a catalyst. Water was used stoichiometrically to the epoxide groups and the second step of the reaction (oxirane ring opening) was carried out at 80 °C. This is a well-established economical route to produce bio-polyols in which double bonds are converted into oxirane moieties, which next are converted into hydroxyl groups by the ring opening reaction using suitable reagents to give a polyol (Pillai et al., 2016). The reaction parameters (solvent type, time and temperature) were optimized in order to produce the most economical and functional bio-polyol. The resulting bio-polyol was marked as PP102.

Polymeric methylene diphenyldiisocyanate (PMDI), containing 31.5 wt.% of free isocyanate groups, was supplied by Minova Ekochem S.A. Polycat 9, an amine based compound produced by Air Products, was used as a catalyst. A silicone surfactant with the trade name Niax Silicone L-6915 produced by Momentive Performance Materials Inc. was used as a stabilizer of the foam structure. Distilled water was used as a "green" chemical blowing agent.

### 2.2. Foam synthesis

Semi-rigid PUR foams with different contents of the PP102 bio-polyol and petrochemical polyol were prepared using a one-step method. The different mass shares of the synthetic polyol were replaced by their bio-polyol equivalents. The formulations are shown in Table 1.

The polyols, amine catalyst, surfactant and water (named "component A") were mechanically stirred for 15 s to ensure their complete homogenization. After that, PMDI (component B) was added to the polyol premix at a NCO/OH molar ratio of 1.1:1.0 (the contributions of the polyols and water were taken into account in the OH calculation) and the whole mixture was mechanically stirred for 5 s and then immediately poured into a plastic container (25 cm × 25 cm × 10 cm).

The nomenclature for the PUR foams contains two parameters: FPP indicating that the foams contain bio-polyol PP102, and 10, 30, 50, 70 or 100 as the information about the bio-polyol content in the polyol premixes. The reference foam based only on the petrochemical polyol was named as REF.

### 2.3. Characterization techniques

#### 2.3.1. Foaming process

In order to analyze the foaming process in details, a FOAMAT® apparatus by Format-Messtechnik GmbH was used. The device can record changes of the temperature, dielectric polarization, pressure and rise velocity of reaction mixtures. Three samples of each formulation were tested. Moreover, the software of the device calculates several parameters such as the start, rise, gelling and curing times, the maximum temperature reached in the PUR system analyzed, etc. The start time is arbitrarily calculated as the time at which the ratio between the instantaneous rise velocity and the maximum rise velocity is 0.15. The gelling time criterion is set as the time at which the dielectric polarization reaches 85% of its maximum value.

#### 2.3.2. The apparent density

The apparent density of the foams was measured by calculating the mass to volume ratio of large foam blocks (about 5 cm × 20 cm × 20 cm), according to ISO 845.

#### 2.3.3. Foam morphology study

Thin films were cut out of the foams using a sharp blade to be observed under an optical microscope (Centrum Mikroskopii, magnification 2.5×). The microphotographs taken (at least 18 images of each sample, 9 cross-sections parallel to the foam rise direction and the other 9 cross-sections perpendicular to the foam rise direction) were analyzed with an ImageJ program. The cellular density of foams was calculated using the following Eq. (1) (Gosselin and Rodrigue, 2005; Rende et al., 2013)

$$N = \left( \frac{n}{A} \right)^{3/2} \quad (1)$$

where  $N$  is the cellular density expressed as the number of cells in a  $\text{cm}^3$ ,  $n$  is the number of cells and  $A$  is the area in the image of a foam cross-section (in the present case it corresponds to  $0.00182 \text{ cm}^2$ ).

#### 2.3.4. Thermal conductivity

Thermal conductivity was measured using a LaserComp heat flow meter instrument and foam samples with dimensions of 5 cm × 20 cm × 20 cm. The thermal conductivity value at an average temperature of 10 °C was measured at the rate of steady state heat transfer across a foam with known thickness, which is induced by two different known temperatures between two opposite surfaces of the foam. In this case, one plate of the equipment was set to 0 °C and the other to 20 °C.

#### 2.3.5. Closed cell content

Closed cell content was measured using a home-made device, according to ISO 4590.

#### 2.3.6. Water absorption

Water absorption was measured according to the ISO 2896 standard, which is based on the Archimedes' principle. The results are expressed as the percentage of water's volume absorbed by a sample.

#### 2.3.7. Dimensional stability

The dimensions of samples of ca. 100 mm × 100 mm × 25 mm were measured in specific positions with a calliper (precision of

**Table 2**

The characteristic of the PP102 and petrochemical polyol.

Property	PP102	Petrochemical polyol
Hydroxyl value (OHV, mg KOH/g)	102.0	449
Acid number (LK, mg KOH/g)	9.0	<0.1
Iodine number (LI, g I <sub>2</sub> /100 g)	7.8	0
Water content (wt.%)	0.12	0.10
Number average molecular weight (Mn)	1648	542
Polydispersity	3.57	4.34
Functionality	3.0	4.3

0.01 mm) and next the samples were conditioned in an oven at 70 °C for 24 h. After that the samples' dimensions were measured again. The dimensional stability was calculated according to ISO 2796-1986 for each sample's dimension as:  $100 * \left( \frac{l_f - l_i}{l_i} \right)$ , where  $l_i$  is the initial measured size and  $l_f$  is the size after the thermal treatment.

#### 2.3.8. Compression tests

The compressive strength of the foams was determined according to ISO 826. The compressive strength was investigated in two directions: parallel and perpendicular to the direction of foam rise. The compressive strength was measured using a Zwick 1445 instrument, at 10% deformation. The compressive force was applied at a speed of 2 mm/s, axially in a perpendicular direction to the square surface.

#### 2.3.9. Thermogravimetric analysis (TGA)

Thermal decomposition curves were obtained using a TGA-50 SHIMADZU thermogravimetric analyzer at a heating rate of 10 °C/min, from 25 °C up to 800 °C under a nitrogen atmosphere.

#### 2.3.10. Dynamic mechanical tests

The dynamic mechanical properties of the samples were determined using an Anton Paar, Physica MCR rheometer. Torsion geometry was used on solid samples with a rectangular shape, whose dimensions were: length = 30 mm, width = 10 mm, thickness = 3 mm. Measurements were performed as temperature sweeps, in the temperature range from –50 to 250 °C at a heating rate of 5 °C/min. The frequency was kept at 1 Hz, and the deformation applied at 1% to ensure working in a linear viscoelastic range. The thermal transition temperatures ( $T_{gs}$ ) were arbitrarily selected as the temperatures of the maxima in the  $\tan \delta$  curves.

### 3. Results and discussion

#### 3.1. Characterization of the bio-polyol

The obtained PP102 bio-polyol was very viscous (almost solid) at room temperature due to the presence of crystals with crystallization temperature slightly over room temperature, like some of bio-based polyols (Kong et al., 2012). The chemical characterization and GPC (Gel Permeation Chromatography) chromatograms of the petrochemical and palm oil-based bio-polyols are shown in Table 2 and Fig. 1, respectively. It is clear that both the average molecular weight and distribution of molecular weights of the bio-polyol are larger than those of the petrochemical one. The iodine value of the PP102 bio-polyol is low but not zero, which indicates that not all the C=C bonds were oxidized during the polyol synthesis. Bio-polyol PP102 had only secondary hydroxyl groups and a relatively low hydroxyl value because oxirane rings during the synthesis were opened using water (Allauddin et al., 2016).

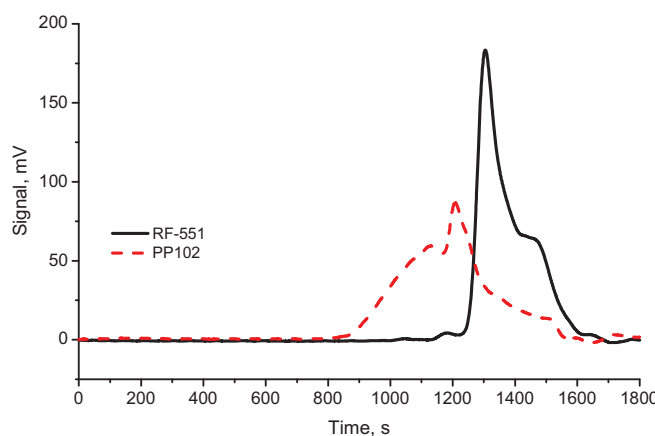


**Fig. 1.** GPC chromatograms of the petrochemical polyol and the palm oil-based bio-polyol.

### 3.2. Foaming kinetics

As indicated in the previous section, the palm oil-derived bio-polyol obtained was solid at room temperature, thus the premix of the polyol components became more viscous as the content of the palm oil-based bio-polyol increased. Moreover, it was noticed that part of this premix tended to precipitate rapidly when the mixture was carried out at room temperature. Therefore, the foaming kinetics was studied in two ways: (a) by mixing all components at room temperature and (b) by blending the premix at 60 °C with the isocyanate component at room temperature. In the second case, firstly, the polyol premix was prepared without a catalyst (to avoid its evaporation during preliminary heating of the polyol premix) and was heated in an oven for 0.5 h at 60 °C. The catalyst was then immediately added to the polyol premix and the mixture was manually stirred for a few seconds.

Fig. 2 shows the dielectric polarization, which reflects the progress of the reactions taking place between functional groups as a function of the reaction time for selected samples. Table 3 summarizes the start and gelling times (calculated by the FOAMAT software) for all the samples tested. The foaming reaction proceeded faster when the premix was heated above room temperature, as expected. Moreover, when the premix was heated it was also possible to prepare FPP100 samples, that is, using the palm oil bio-polyol as the unique polyol. On the other hand, it was noticed that the differences in the reactivity of the samples due to their mixing temperature were minimal when just the petrochemical polyol was used, but increased considerably as the amount of PP102 was added to the PUR system. This behaviour is attributed to two opposite effects: the lower viscosity of the systems mixed at a higher temperature that allowed the exothermic reaction to initiate faster and the lower reactivity of the bio-polyol in comparison with that of the petrochemical one that led to a decrease of the system reactivity as the PP102 content increased. The last effect can be clearly noticed in Fig. 2 by comparing the curves obtained at the same initial temperature. The dielectric polariza-

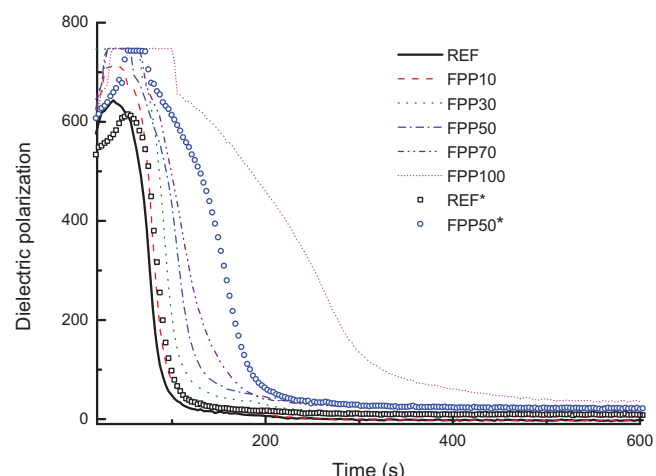


**Fig. 2.** Dielectric polarization of different PUR systems modified with bio-polyol PP102 as a function of the reaction time.

tion decreases more gradually as the concentration of the PP102 bio-polyol increases indicating that the consumption of functional groups (such as isocyanate and hydroxyl ones) occurs more slowly. This is attributed to the secondary hydroxyl groups in the palm oil bio-polyol that result in strong steric hindrance as compared with the primary hydroxyl groups of the petrochemical polyol (Campanella et al., 2009; Kurańska and Prociak, 2016). Moreover, the palm oil bio-polyol used in this work has a low hydroxyl value in comparison with the petrochemical polyol which affects its reactivity too. This behaviour is in agreement with similar works reported in literature (Hu et al., 2002; Zhou et al., 2015). The averaged start and gelling times reported in Table 3 confirm the previous observations.

### 3.3. Physical properties and foam structure

The apparent density, content of closed cells and thermal conductivity of the foams modified with palm oil bio-polyol are reported in Table 4. The replacement of the petrochemical polyol with the PP102 bio-polyol caused a decrease of the apparent density of the foams obtained, with the exception of the FPP100 sample that deviates from this trend. Such an effect could be associated with lower reactivity of the systems modified with the bio-polyol, which retarded the gelling of the foam and thus the cells were able to increase their volumes during a longer time. Moreover, a longer foam expansion time could also cause cracking of cells. A confirmation of this effect is the significantly lower content of closed cells in the foams modified with the palm oil-based bio-polyol respect to that of the REF foam, which also decreased as the content of the PP102 bio-polyol increased.

Regarding thermal conductivity, it is important to remark that the main use of rigid foams is for heat insulating applications (Tan et al., 2011; Septevani et al., 2015) and thus, it is essential to keep this value as low as possible. The thermal conductivity of foams is influenced mainly by three factors: the conductivity of the PUR

**Table 3**

The characteristic times of the foaming processes of the reference and modified PUR systems.

Foam symbol/foaming parameter	REF	FPP10	FPP30	FPP50	FPP70	FPP100
<b>Premix at 20 °C</b>						
Start time (s)	16.7 ± 1.8	16.5 ± 1.4	20.4 ± 0.1	20.4 ± 2.1	30.4 ± 2.2	-
Gelling time (s)	37.6 ± 0.9	35.9 ± 1.9	41.1 ± 2.3	41.9 ± 1.4	50.4 ± 2.6	-
<b>Premix at 60 °C</b>						
Start time (s)	14.7 ± 1.8	15.5 ± 0.1	17.1 ± 2.3	15.5 ± 0.1	15.5 ± 0.1	24.3 ± 3.3
Gelling time (s)	23.8 ± 2.1	41.7 ± 17.5	36.0 ± 22.6	26.5 ± 8.4	27.0 ± 4.1	34.3 ± 1.1

**Table 4**

Apparent density, content of closed cells and thermal conductivity of the reference sample and foams modified with palm oil bio-polyol.

Foam symbol	Apparent density, kg/m <sup>3</sup>	Content of closed cells, %	Thermal conductivity, mW/m·K
REF	34.9 ± 0.8	83.4 ± 4.0	24.9 ± 1.4
FPP10	33.3 ± 0.2	58.0 ± 16.9	30.0 ± 3.3
FPP30	32.1 ± 0.8	49.4 ± 17.5	30.6 ± 1.0
FPP50	29.7 ± 1.0	10.7 ± 7.06	33.1 ± 1.5
FPP70	29.4 ± 1.8	8.9 ± 1.5	35.5 ± 1.1
FPP100	49.8 ± 2.8	—	40.0 ± 2.2

**Table 5**

Foams' morphology.

Foam symbol	Transversal direction				Rise direction			
	NC	CC × 10 <sup>3</sup>	An	N × 10 <sup>-5</sup>	NC	CC × 10 <sup>3</sup>	An	N × 10 <sup>-5</sup>
REF	43.96 ± 8.35	4.53 ± 1.09	1.02 ± 0.06	2.95 ± 0.83	22.3 ± 2.95	3.34 ± 0.70	1.13 ± 0.03	1.06 ± 0.29
FPP10	76.51 ± 6.57	2.12 ± 0.16	1.19 ± 0.04	6.71 ± 0.88	46.29 ± 9.47	3.34 ± 0.70	1.14 ± 0.03	3.19 ± 0.99
FPP30	59.13 ± 9.72	3.42 ± 0.84	1.18 ± 0.05	4.59 ± 1.09	43.89 ± 4.84	4.90 ± 1.01	1.59 ± 0.05	2.92 ± 0.46
FPP50	54.33 ± 9.91	3.74 ± 0.88	1.30 ± 0.09	4.05 ± 1.08	55.56 ± 7.44	3.53 ± 1.15	1.37 ± 1.15	4.17 ± 0.82
FPP70	38.03 ± 4.72	4.80 ± 0.80	1.66 ± 0.07	2.36 ± 0.44	24.79 ± 3.77	6.01 ± 2.29	1.25 ± 0.12	1.24 ± 0.28

NC, number of cells per mm<sup>2</sup>; CC, cell cross-section area (mm<sup>2</sup>); An, anisotropy index; N, cell density, (number of cells/cm<sup>3</sup>).



Fig. 3. Optical image of the FPP100 foam (cross-section).

phase as well as the gas trapped (CO<sub>2</sub> in this case) within the closed cell structure (Mosiewicki et al., 2009; Tan et al., 2011; Septevani et al., 2015), and the heat transport by radiation between cells (Septevani et al., 2015). According to Septevani et al. (2015), who analyzed the previous contributions in terms of the cell size and closed cell content, both characteristics are strongly correlated with the thermal conductivity in opposite ways: the thermal conductivity of foams increases with an increasing cell size but decreases with an increasing closed cell content, as can also be confirmed by the results shown in Table 4. The results found in this work also agree with the conclusions of Tan et al. (2011) who demonstrated that thermal conductivity is closely related to the foam density and cell morphology. It was concluded that a low conductivity results from a low foam density, a small average cell size and a high closed cell content. From the results obtained in this work it is clear that the closed cell content considerably depends on the bio-polyol content in PUR systems and strongly influences the foams' thermal conductivity. Open cells allow more convection, and even air to enter the foam which has a much higher conductivity value (24.9 mW/(mK)) than that of CO<sub>2</sub> (15.3 mW/(mK)) (Tan et al., 2011).

On the other hand, the foam prepared using only palm bio-polyol needs to be considered separately. Its start time was considerably longer than those of the other samples and the maximum temperature reached during the reaction considerably lower, thus the viscosity of the reacting system was higher than in the other cases. This influenced inadequately the resulting foam morphology leading to a heterogeneous sample with zones having large pores (collapsed cells) and others with very small cells (Fig. 3). Thus, this sample was discarded from further analysis (Fig. 4).

**Table 6**

Water absorption (WA) and dimensional stability (DS) of the foams: reference and modified with palm oil bio-polyol.

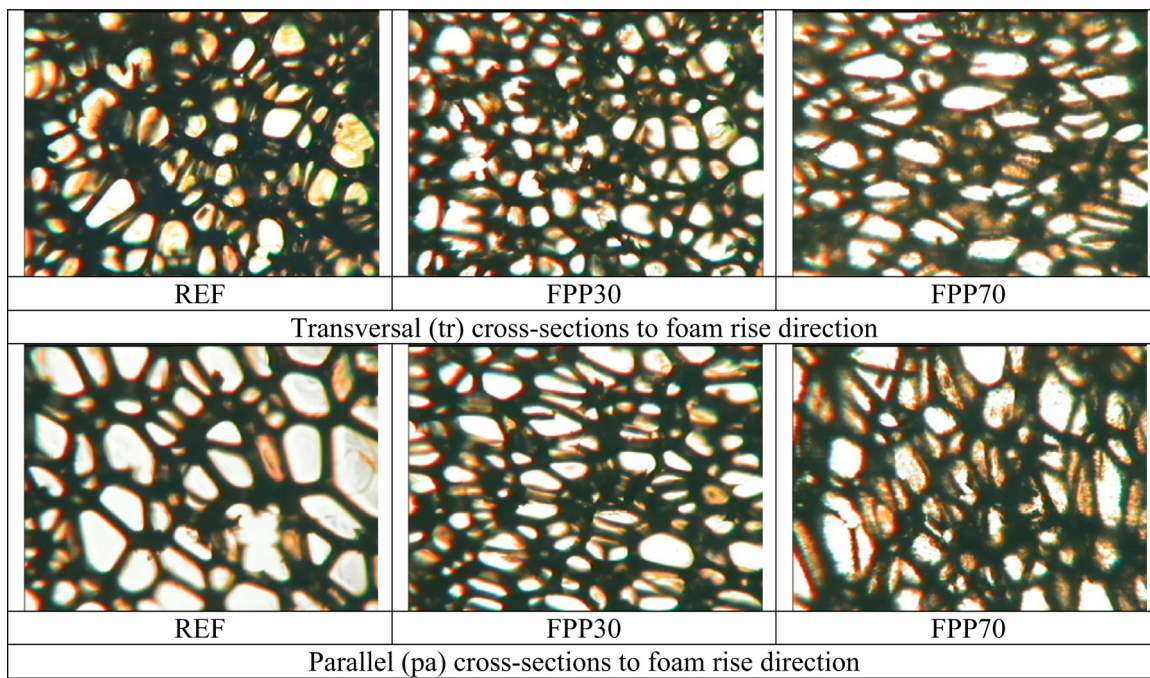
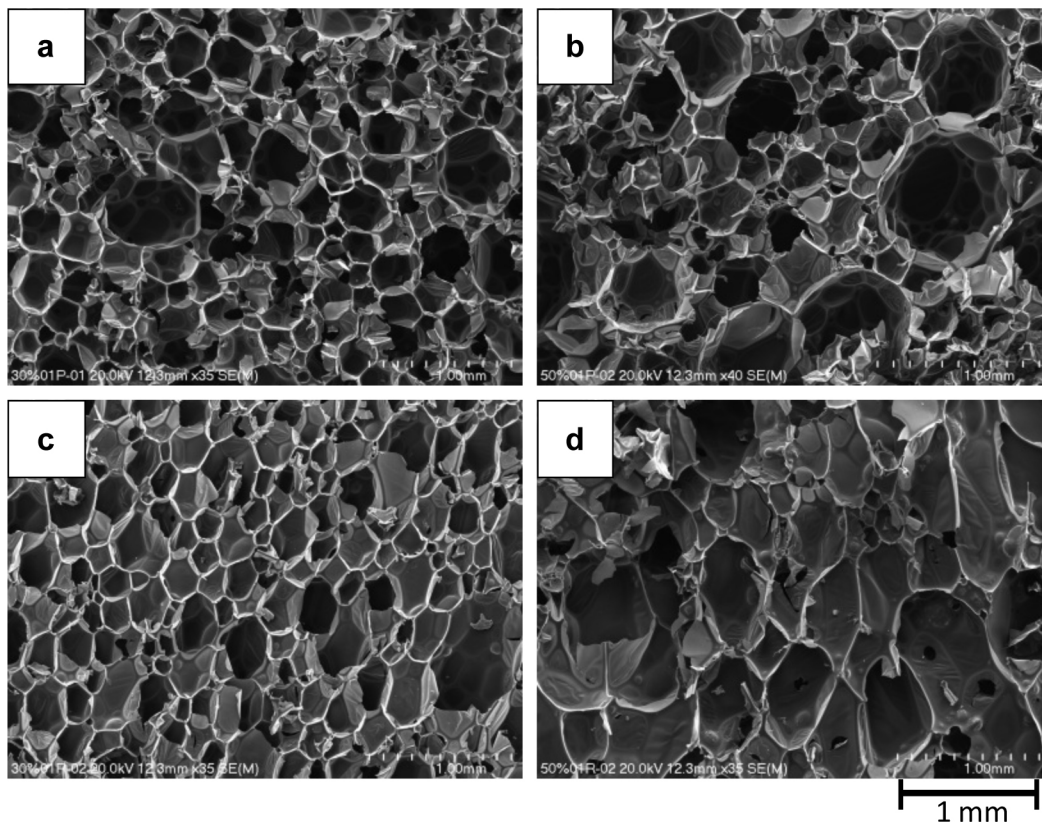
Foam symbol	DSy (%)	DSx (%)	DSz (%)	WA (% g/cm <sup>3</sup> )
REF	0.08 ± 0.14	0.08 ± 0.18	-0.03 ± 0.39	1.12 ± 0.37
FPP10	-0.07 ± 0.22	-0.09 ± 0.05	0.13 ± 0.71	0.64 ± 0.07
FPP30	0.02 ± 0.53	-0.18 ± 0.14	0.34 ± 0.32	0.17 ± 0.03
FPP50	-0.37 ± 0.17	-0.13 ± 0.05	-0.35 ± 0.55	0.34 ± 0.08
FPP70	-0.27 ± 0.20	-0.35 ± 0.55	0.01 ± 0.36	0.53 ± 0.27

The cell structures shown in Fig. 5 are typical of the foams prepared in this work. The characteristics such as the number of cells, cell size (cross-section surface), density and anisotropy were determined using an image analysis of optical micrographs (Table 5). It is clear that the number of cells in the selected area of the modified foams (containing up to 50% of the bio-polyol) is higher than that of the reference sample. However, the trend reverses for the sample prepared using 100 wt.% of the bio-polyol (FPP100). Since the number of cells in the selected area is inversely proportional to the cell cross-section area, the trend in these values is approximately the opposite. The anisotropy of the cells clearly increases with the palm bio-polyol content for the cross-sections in the transversal direction, but does not exhibit a clear trend for the cross-sections parallel to the foam expansion direction. The same behaviour is noticed for the cell density. To summarize, the replacement of the petrochemical polyol with the bio-derived one led to less homogeneous and more anisotropic foams, as can also be confirmed by the morphology shown in the SEM pictures of Fig. 5.

Regarding dimensional stability, in all cases the variations in the sample's dimensions after the thermal treatment are random (Table 6). Sometimes an increase in the dimensions is observed, at other times there is a decrease; however the changes are negligible if compared with the standard deviation, and thus they can be attributed mostly to experimental errors while measuring. Concerning water absorption, it is remarkable that the modified foams absorb less water than the reference material even though the amount of water absorbed per unit volume is really low.

### 3.4. Compression properties

The compression properties of the foams are presented in Table 7. As expected, both the modulus and compressive strength decrease as the content of the palm oil-based bio-polyol in the PUR formulation increases. Moreover, both the modulus and compres-

**Fig. 4.** Optical photographs of selected foams.**Fig. 5.** SEM microphotographs of selected foams: (a) FPP30, transversal direction; (b) FPP50, transversal direction; (c) FPP30, parallel direction; (d) FPP50, parallel direction.

sive strength for the samples tested perpendicularly to the foam rise direction (transversal) are lower than the corresponding values measured parallel to the foam rise direction. These results are an effect of the anisotropic character of the foams obtained. The mechanical properties of PUR foams are closely correlated with their apparent density ([Mosiewicki et al., 2009](#); [Septevani et al.,](#)

[2015](#)). However, in the present case, the reduction in the apparent density of the bio-based foams is not enough to justify the decrease in the compression properties reported in [Table 7](#), i.e. the apparent density of FPP70 is 0.84 times that of the REF sample, while its parallel modulus and compression strength are just 0.69 and 0.54, respectively, as compared to the REF foam.

**Table 7**

The compression properties of the foams modified with the palm oil bio-polyol.

Foam symbol	Parallel		Transversal	
	Modulus (MPa)	Strength at 10% deformation	Modulus (MPa)	Strength at 10% deformation
REF	5.54 ± 0.76	187.2 ± 16.7	3.34 ± 0.36	125.2 ± 9.9
FPP10	5.11 ± 1.15	181.3 ± 11.4	3.36 ± 0.35	140.0 ± 9.4
FPP30	3.73 ± 1.23	154.3 ± 12.0	2.20 ± 0.48	114.6 ± 12.0
FPP50	4.43 ± 0.46	141.4 ± 11.1	1.88 ± 0.16	87.5 ± 7.1
FPP70	3.80 ± 0.20	100.5 ± 37.6	1.22 ± 0.16	59.3 ± 5.9

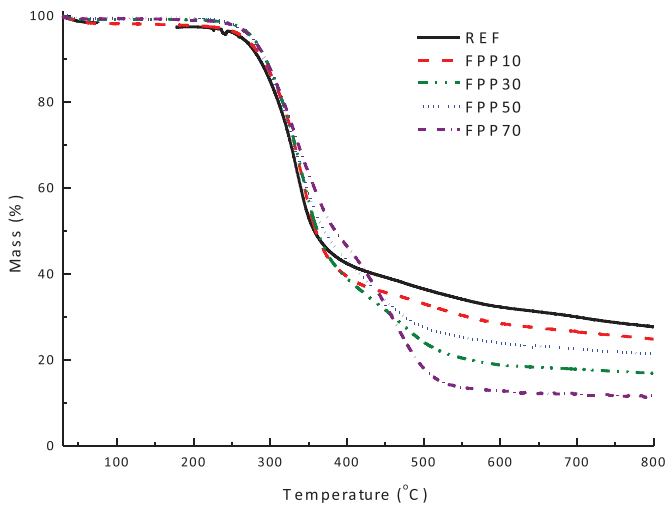


Fig. 6. Thermal degradation patterns of selected foams.

The compression of the foams starts in the linear elastic region (where stress is linearly proportional to deformation). In this zone elasticity is controlled by cell wall bending, and, in the case of closed cells, by stretching of the cell walls. The modulus value is calculated from the slope of the stress vs. strain curve in this region. On the other hand, higher applied stress leads to a collapse or cell buckling of the foams to finally result in an irreversible damage of the cell walls (densification region) (Pillai et al., 2016). Thus, the results obtained in this work can be attributed to the different formulations of the foams: the increasing amounts of dangling chains added to the relatively reduced content of primary hydroxyl groups as the concentration of the bio-polyol increases lead to weaker cell walls (Septevani et al., 2015). In this sense, weaker cell walls would bend at lower loads than stronger ones, causing lower compression modulus values. The reduction of the content of closed cells with an increasing addition of palm-based bio-polyol also contributes to these results due to the modulus coming from the stretching of the closed cell walls, which is decreased as the bio-polyol content increases. The tendency described is disordered in the case of modulus values for the foams FPP30, FPP50 and FPP70, measured parallel to the foam rise direction. It was probably an effect of differences in the cell size. For the foams mentioned, the modulus changes are correlated with the foam cell size in the cross-section parallel to the foam rise direction (Table 5). In the case of foam FPP50, the cell density as well as modulus value (for the direction parallel to the foams' rise direction) were noticed to be the highest among the compared foams FPP30, FPP50 and FPP70.

The thermal stability of the prepared foams is shown in Fig. 6. The weight lost for the samples up to 250 °C corresponds to the moisture absorbed by the foams and thus depends on the initial content of the bio-polyol in each sample. It can be seen that the foams containing no or small amounts of the bio-polyol have two stages of degradation during the heating process, while 3-stage degradation can be clearly identified for the FPP50 and FPP70 sam-

ples. All the foams present essentially the same degradation pattern up to about 325 °C. Between 325 and 440 °C, the samples containing 50 and 70 wt.% of the bio-polyol in the polyol premix degrade at a lower rate than the ones with a smaller content of the bio-polyol. In this whole range (i.e. from 250 to 440 °C) the weight loss is attributed to the degradation of the urethane linkages (Septevani et al., 2015) followed by polyol decomposition (Septevani et al., 2015; Zhou et al., 2015) and thus the differences between the samples correspond to the different relative contents of the petrochemical polyol and the palm bio-polyol. The urethane linkage degradation involves three competing mechanisms: the dissociation of the original isocyanates and polyol precursors, the formation of carbamic acid and olefin with subsequent carbamic acid dissociation to primary amine and carbon dioxide and the formation of secondary amine and carbon dioxide (Septevani et al., 2015). These three reactions occur simultaneously and the prevalence of each process is dependent on the structure of the urethane and the reaction conditions. At higher temperatures the degradation of the isocyanate component of the foams takes place, as reported by Zhou et al. (2015) in association with the depolycondensation and polyol degradation (Septevani et al., 2015). Moreover, it is clear that the residual char is dependent on the foam's composition and decreased from about 28% (800 °C, the REF foam) to 12% (800 °C, the FPP70 sample), as reported in similar works (Zieleniewska et al., 2015).

The dynamic mechanical behaviour of the foams as function of temperature is presented in Fig. 7a and b. It can be noticed that the storage modulus ( $G'$ ) decreases as the content of the bio-polyol increases, confirming the compression behaviour. The higher  $G'$  for the reference foam was due to its higher apparent density, as well as higher cross-linking density than for those modified with the palm oil-based bio-polyol. As the petrochemical polyol substitution increased, glassy to rubbery transition took place gradually to higher temperatures, although almost no changes were observed for the bio-polyol contents in the polyol premixes lower than 30 wt.%. No rubbery plateau was observed for any of the foams in the range of temperatures analyzed. The main thermal glass-rubber transitions ( $T_{gs}$ ), determined from the peak in  $\tan \delta$  increased from about 205 °C (0–30% palm bio-polyol) to 217 °C (50% palm bio-polyol) and about 230 °C for the FPP70 sample. With an increasing petrochemical polyol substitution, the  $\tan \delta$  peak broadened, indicating increased network inhomogeneity consistent with the heterogeneity of the bio-polyol employed. Similar results were found by Tan et al. (2011), Ribeiro da Silva et al. (2013) and Septevani et al. (2015), among others.

#### 4. Conclusions

In summary, semi-rigid polyurethane foams were successfully prepared by blending up to 70 wt.% of a palm oil-based bio-polyol with a petrochemical polyether polyol. An analysis of selected parameters of the foaming processes showed a slight deceleration in the foaming and gelling reactions as an effect of an increase of the content of the palm oil-based bio-polyol in the formulations that

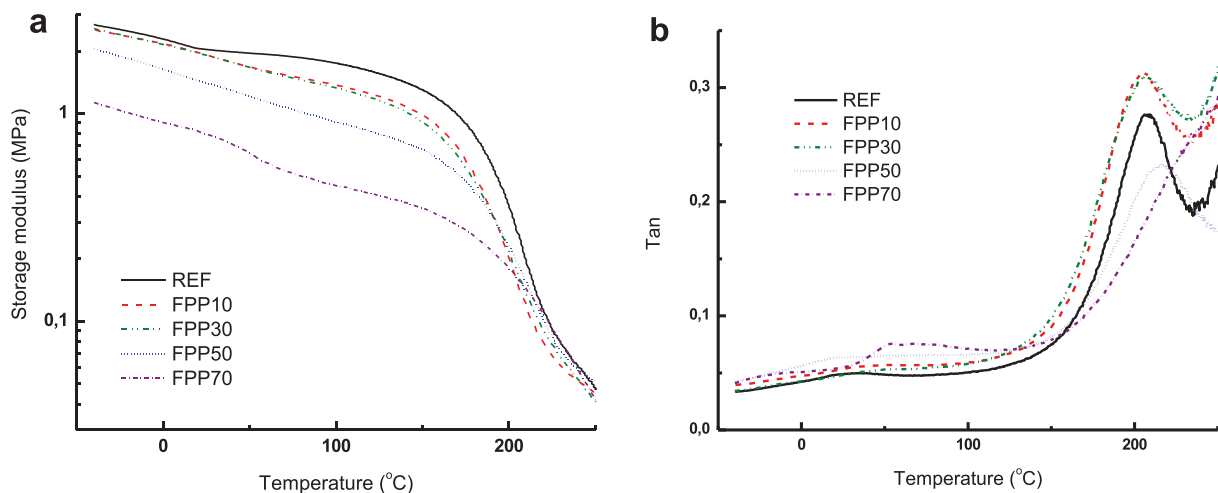


**Fig. 7.** Dynamic mechanical behaviour of the bio-foams. (a) Storage modulus vs. temperature; (b)  $\tan \delta$  vs. temperature.

were attributed to the low hydroxyl value and content of secondary hydroxyl groups of the bio-polyol.

The unfavourable changes of thermal conductivity are an effect of the foam's cellular structure, mainly attributed to the closed cell content that decreases as the amount of the palm oil-based bio-polyol in the formulation increases. However, the water absorption decreases as the bio-polyol concentration in the PUR formulation increases and the open cell structure in this type of heat insulating boards allows easier migration of moisture.

The modified foams presented an excellent dimensional stability although the compression properties and the storage modulus decreased as the palm oil-based bio-polyol content increased. The thermal stability of the modified foams is adversely affected only at temperatures higher than 325 °C. The increased bio-polyol content in the polyurethane system leads to a decrease of the residual char after a thermogravimetric measurement.

## Acknowledgments

The research has financial support in the frame of The People Programme (Marie Curie Actions – International Research Staff Exchange Scheme) of the European Union's Seventh Framework Programme under the REA grant agreement n° PIRSES-GA-2012-318996 titled "Bio-based polyurethane composites with natural fillers" (Acronym: BIOPURFIL).

The authors are also grateful to Momentive Performance Materials for supplying the surfactants.

## References

- Allauddin, S., Somisetti, V., Ravinder, T., Rao, B.V.S.K., Narayan, R., Raju, K.V.S.N., 2016. One-pot synthesis and physicochemical properties of high functionality soy polyols and their polyurethane-Urea coatings. *Ind. Crop. Prod.* 85, 361–371.
- Arbenz, A., Frache, A., Cuttica, F., Averous, L., 2016. Advanced biobased and rigid foams, based on urethane-modified isocyanurate from oxypropylated gambier tannin polyol. *Polym. Degrad. Stab.* 132, 62–68.
- Arniza, M.Z., Hoong, S.S., Idris, Z., Yeong, K.S., Hassan, H.A., Din, A.K., Choo, Y.M., 2015. Synthesis of transesterified palm olein-based polyol and rigid polyurethanes from this polyol. *J. Am. Oil. Chem. Soc.* 92, 243–255.
- Arshanitsa, A., Krumina, L., Telysheva, G., Dizhbite, T., 2016. Exploring the application potential of incompletely soluble organosolv lignin as a macromonomer for polyurethane synthesis. *Ind. Crop. Prod.* 92, 1–12.
- Bernardini, J., Cinelli, P., Anguillesi, I., Coltellini, M., Lazzeri, A., 2015. Flexible polyurethane foams green production employing lignin or oxypropylated lignin. *Eur. Polym. J.* 64, 147–156.
- Calvo-Correas, T., Martin, M.D., Retegi, A., Gabilondo, N., Corcuera, M.A., Eceiza, A., 2016. Synthesis and characterization of polyurethanes with high renewable carbon content and tailored properties. *ACS Sustain. Chem. Eng.* 4, 5684–5692.
- Calvo-Correas, T., Mosiewicki, M.A., Corcuera, M., Eceiza, A., Aranguren, M.I., 2015. Linseed oil-based polyurethane rigid foams: synthesis and characterization. *J. Renew. Mater.* 3, 3–13.
- Campanella, L.M., Bonnaillie, R.P., Wool, R.P., 2009. Polyurethane foams from soyoil-based polyols. *J. Appl. Polym. Sci.*, 112.
- Cateto, C.A., Barreiro, M.F., Rodrigues, A.E., Belgacem, M.N., 2011. Kinetic study of the formation of lignin-based polyurethanes in bulk. *React. Funct. Polym.* 71, 863–869.
- Cateto, C.A., Barreiro, M.F., Rodrigues, A.E., Belgacem, M.N., 2009. Optimization study of lignin oxypropylation in view of the preparation of polyurethane rigid foams. *Ind. Eng. Chem. Res.* 48, 2583–2589.
- D'Souza, J., Camargo, R., Yan, N., 2014. Polyurethane foams made from liquefied bark based polyols. *J. Appl. Polym. Sci.*, 131.
- Gomez-Fernandez, S., Ugarte, L., Pena-Rodriguez, C., Corcuera, M.A., Eceiza, A., 2016. The effect of phosphorus containing polyol and layered double hydroxides on the properties of a castor oil based flexible polyurethane foam. *Polym. Degrad. Stab.* 132, 41–51.
- Gosselin, R., Rodriguez, D., 2005. Cell morphology analysis of high density polymer foams. *Polym. Test.* 24, 1027–1035.
- Hakim, A.A., Nassar, M., Emam, A., Sultan, M., 2011. Preparation and characterization of rigid polyurethane foam prepared from sugar-cane bagasse polyol. *Mater. Chem. Phys.* 129, 301–307.
- Hu, Y.H., Gao, Y., Wang, D.N., Hu, C.P., Zu, S., Vanoverloop, L., Randall, D., 2002. Rigid polyurethane foam prepared from a rape seed oil based polyol. *J. Appl. Polym. Sci.* 84, 591–597.
- Kirpluks, M., Cabulis, U., Kurańska, M., Prociak, A., 2013. Three different approaches for polyol synthesis from rapeseed oil. *Key Eng. Mater.* 559, 69–74.
- Kong, X., Liu, G., Curtis, J.M., 2012. Novel polyurethane produced from canola oil based poly(ether ester) polyols: synthesis, characterization and properties. *Eur. Polym. J.* 48, 2097–2106.
- Kurańska, M., Prociak, A., Kirpluks, M., Cabulis, U., 2013. Porous polyurethane composites based on bio-components. *Comp. Sci. Technol.* 11, 70–76.
- Kurańska, M., Prociak, A., Kirpluks, M., Cabulis, U., 2015a. Polyurethane–polysisocyanurate foams modified with hydroxyl derivatives of rapeseed oil. *Ind. Crop. Prod.* 74, 849–857.
- Kurańska, M., Prociak, A., Cabulis, U., Kirpluks, M., 2015b. Water-blown polyurethane–polysisocyanurate foams based on bio-polyols with wood fibers. *Polimery* 60, 705–712.
- Kurańska, M., Prociak, A., 2016. The influence of rapeseed oil-based polyols on the foaming process of rigid polyurethane foams. *Ind. Crop. Prod.* 89, 182–187.
- Lee, C.S., Ooi, T.L., Chuan, C.H., Ahmad, S., 2007. Rigid polyurethane foam production from palm oil-based epoxidized diethanolamides. *J. Am. Oil. Chem. Soc.* 84, 1161–1167.
- Malewska, E., Bąk, S., Prociak, A., 2015. Effect of different concentration of rapeseed-oil-based polyol and water on structure and mechanical properties of flexible polyurethane foams. *J. Appl. Polym. Sci.*, 132.
- Mosiewicki, M.A., Dell'Arciprete, G.A., Aranguren, M.I., Marcovich, N.E., 2009. Polyurethane foams obtained from castor oil-based polyol and filled with wood flour. *J. Compos. Mater.* 43, 3057–3072.
- Mosiewicki, M.A., Casado, U., Marcovich, N.E., Aranguren, M.I., 2008. Vegetable oil based-polymers reinforced with wood flour. *Mol. Cryst. Liquid Cryst.* 484, 143–150.
- Oliveira, F., Ramires, E.C., Frollini, W., Belgacem, M.N., 2015. Lignopolyurethanic materials based on oxypropylated sodium lignosulfonate and castor oil blends. *Ind. Crop. Prod.* 72, 77–86.
- Paberza, A., Cabulis, U., Arshanitsa, A., 2014. Wheat straw lignin as filler for rigid polyurethane foams on the basis of tall oil amide. *Polimery* 59, 477–481.
- Pawlak, H., Prociak, A., 2012. Influence of palm oil-based polyol on the properties of flexible polyurethane foams. *J. Polym. Environ.* 20, 438–445.

- Pillai, P.K.S., Li, S., Bouzidi, L., Narine, S.S., 2016. Metathesized palm oil & novel polyol derivatives: structure, chemical composition and physical properties. *Ind. Crop. Prod.* 84, 205–223.
- Prociak, A., Kurańska, M., Malewska, E., Szczepkowski, L., Zieleniewska, M., Ryszkowska, J., Ficoń, J., Rząsa, A., 2015. *Polimery* 60, 71–78.
- Prociak, A., Rojek, P., Pawlik, H., 2012. Flexible polyurethane foams modified with natural oil based polyols. *J. Cell. Plast.*, 12.
- Prociak, A., Rojek, P., 2012. Effect of different rapeseed-oil-based polyols on mechanical properties of flexible polyurethane foams. *J. Appl. Polym. Sci.*, 125.
- Rende, D., Schadler, L.S., Ozisik, R., 2013. Controlling foam morphology of poly(methyl methacrylate) via surface chemistry and concentration of silica nanoparticles and supercritical carbon dioxide process parameters. *J. Chem.*, 1–13, 864926.
- Ribeiro da Silva, V., Mosiewicki, M.A., Yoshida, M.I., Coelho da Silva, M., Stefani, P.M., Marcovich, N.E., 2013. Polyurethane foams based on modified tung oil and reinforced with rice husk ash II: mechanical characterization. *Polym. Test.* 32, 665–672.
- Septevani, A.A., Evans, D.A.C., Chaleat, C., Martin, D.J., Annamalai, P.K., 2015. A systematic study substituting polyether polyol with palm kernel oil based polyester polyol in rigid polyurethane foam. *Ind. Crop. Prod.* 66, 16–26.
- Seydibeyoglu, M.O., Misra, M., Mohanty, A., Blaker, J.J., Lee, K., Bismarck, A., Kazemizadeh, M., 2013. Green polyurethane nanocomposites from soy polyol and bacterial cellulose. *J. Mater. Sci.* 48, 2167–2175.
- Soto, G.D., Marcovich, N.E., Mosiewicki, M.A., 2016. Flexible polyurethane foams modified with biobased polyols: synthesis and physical-chemical characterization. *J. Appl. Polym. Sci.*, 15.
- Tan, S., Abraham, T., Ference, D., Macosko, C.W., 2011. Rigid polyurethane foams from a soybean oil-based polyol. *Polymer* 52, 2840–2846.
- Tanaka, R., Hirose, S., Hatakeyama, H., 2008. Preparation and characterization of polyurethane foams using a palm oil-based polyol. *Bioresour. Technol.* 99, 3810–3816.
- Yao, Y., Yoshioka, M., Shiraishi, N., 1996. Water-absorbing polyurethane foams from liquefied starch. *J. Appl. Polym. Sci.* 60, 1939–1949.
- Zeimaran, E., Kadir, M.R., Nor, H.M., Kamarul, T., Djordjevic, I., 2013. Synthesis and characterization of polyacids from palm acid oil and sunflower oil via addition reaction. *Bioorg. Med. Chem. Lett.* 23, 6616–6619.
- Zhang, C., Kessler, M.R., 2015. Bio-based polyurethane foam made from compatible blends of vegetable-oil-based polyol and petroleum-based polyol. *ACS Sustain. Chem. Eng.* 3, 743–749.
- Zhou, X., Sain, M.M., Oksman, K., 2015. Semi-rigid biopolyurethane foams based on palm-oil polyol and reinforced with cellulose nanocrystals. *Compos. A* 83, 56–62.
- Zieleniewska, M., Leszczyński, M.K., Kurańska, M., Prociak, A., Szczepkowski, L., Krzyżowska, M., Ryszkowska, J., 2015. Preparation and characterization of rigid polyurethane foams using a rapeseed oil-based polyol. *Ind. Crop. Prod.* 74, 887–897.